Acta Biomaterialia 13 (2015) 324–334

Contents lists available at ScienceDirect

Acta Biomaterialia

journal homepage: www.elsevier.com/locate/actabiomat

Carbon-nanotube-interfaced glass fiber scaffold for regeneration of transected sciatic nerve

Hong-Sun Ahn [a,b,1], Ji-Young Hwang [b,1], Min Soo Kim [a,b], Ja-Yeon Lee [a,b], Jong-Wan Kim [a,b], Hyun-Soo Kim [a,b], Ueon Sang Shin [b], Jonathan C. Knowles [a,c], Hae-Won Kim [a,b,d,*], Jung Keun Hyun [a,b,e,*]

[a] Department of Nanobiomedical Science and BK21 PLUS NBM Global Research Center for Regenerative Medicine, Dankook University, Cheonan 330-714, Republic of Korea
[b] Institute of Tissue Regeneration Engineering, Dankook University, Cheonan 330-714, Republic of Korea
[c] Division of Biomaterials and Tissue Engineering, Eastman Dental Institute, University College London, 256 Gray's Inn Road, London WC1X 8LD, UK
[d] Department of Biomaterial Science, School of Dentistry, Dankook University, Cheonan 330-714, Republic of Korea
[e] Department of Rehabilitation Medicine, College of Medicine, Dankook University, Cheonan 330-714, Republic of Korea

ARTICLE INFO

Article history:
Received 24 July 2014
Received in revised form 5 November 2014
Accepted 13 November 2014
Available online 21 November 2014

Keywords:
Carbon nanotubes
Peripheral nerve regeneration
Phosphate glass fibers
Scaffold
Sciatic nerve

ABSTRACT

Carbon nanotubes (CNTs), with their unique and unprecedented properties, have become very popular for the repair of tissues, particularly for those requiring electrical stimuli. Whilst most reports have demonstrated in vitro neural cell responses of the CNTs, few studies have been performed on the in vivo efficacy of CNT-interfaced biomaterials in the repair and regeneration of neural tissues. Thus, we report here for the first time the in vivo functions of CNT-interfaced nerve conduits in the regeneration of transected rat sciatic nerve. Aminated CNTs were chemically tethered onto the surface of aligned phosphate glass microfibers (PGFs) and CNT-interfaced PGFs (CNT–PGFs) were successfully placed into three-dimensional poly(L/D-lactic acid) (PLDLA) tubes. An in vitro study confirmed that neurites of dorsal root ganglion outgrew actively along the aligned CNT–PGFs and that the CNT interfacing significantly increased the maximal neurite length. Sixteen weeks after implantation of a CNT–PGF nerve conduit into the 10 mm gap of a transected rat sciatic nerve, the number of regenerating axons crossing the scaffold, the cross-sectional area of the re-innervated muscles and the electrophysiological findings were all significantly improved by the interfacing with CNTs. This first in vivo effect of using a CNT-interfaced scaffold in the regeneration process of a transected rat sciatic nerve strongly supports the potential use of CNT-interfaced PGFs at the interface between the nerve conduit and peripheral neural tissues.

1. Introduction

Peripheral nerve injury is frequently encountered in the clinical setting. An injured peripheral nerve can regenerate spontaneously, but the regenerative capacity is limited in long defects and severe injury [1]. Current medical and surgical management techniques, including autologous nerve grafts and allografts, are in most cases not sufficient for complete regeneration of the damaged peripheral nerve [2]. Artificial nerve conduits, such as single hollow tubes, are commercially available for the connection of transected peripheral nerves, but are not thought to be suitable as a physical guide for the regeneration of a long defect [3]. Many types of scaffold configuration and fabrication, including intraluminal microchannel formation [4] and electrospun nanostructured scaffolds [5,6], have been attempted to give physical and biological cues for outgrowing axons and to overcome the limitations of regeneration in the peripheral nervous system. The delivery of growth factors [7], pharmacological agents [8], stem cells [9] or Schwann cells [10] within the nerve conduit might be other options for improving neural regeneration [11,12].

Intraluminal structures for physical guidance of outgrowing axons have been developed using collagen fibers [13], denatured muscle tissue [14] and aligned phosphate glass fiber (PGF) bundles [15], though the results thus far have proved unsatisfactory.

Carbon nanotubes (CNTs) have unique chemical, mechanical, structural and electrical properties that make them attractive for the repair and regeneration of tissues, including nerves, and functionalized CNTs have also been applied to stroke and spinal cord injury models [16–18]. A body of key literature has already demonstrated the significant and profound effects of CNTs,

* Corresponding authors at: Department of Nanobiomedical Science and BK21 PLUS NBM Global Research Center for Regenerative Medicine, Dankook University, Cheonan 330-714, Republic of Korea. Tel.: +82 41 550 3081; fax: +82 41 559 7840 (H.-W. Kim). Tel.: +82 41 550 3889; fax: +82 41 551 7062 (J.K. Hyun).
E-mail addresses: kimhw@dku.edu (H.-W. Kim), rhhyun@dankook.ac.kr (J.K. Hyun).
[1] These authors contributed equally to this work.

http://dx.doi.org/10.1016/j.actbio.2014.11.026
1742-7061/

particularly on nerve cells and even stem cells, with regard to their neurite outgrowth and neuronal differentiation [19–23], and CNT-based substrates have been suggested as potential agents for the stimulation of neuronal functions and the repair and regeneration of damaged and diseased neural tissues [18,24]. The nanotopographical and biochemical features and electrical conductivity of CNTs may mediate neural modulation [25]. Therefore, CNTs are expected to have synergistic effects on peripheral nerve regeneration when interfaced with an intraluminar structured scaffold. However, most of the studies mentioned were performed in vitro, and there is little evidence about the in vivo functions of CNT-interfaced biomaterials in nerve damage models.

Therefore, we show here for the first time the in vivo effects of CNT-interfaced substrates on nerve regeneration using a transected rat sciatic nerve model. For this, we chemically linked functionalized CNTs onto the surface of aligned PGF bundles, aiming at utilizing CNTs as an interfacing material while the aligned fiber bundles are expected to function for physical guidance. Our previous studies on PGF have shown that aligned PGFs within a collagen scaffold were effective in guiding nerve tissues in a transected rat sciatic nerve model as well as in a transected rat spinal cord injury model [15]. PGFs, a class of optical glasses composed of metaphosphates of various metals, offer biocompatibility and tailored directionality; as such, they are considered to be suitable for the regeneration of tissues requiring directional guidance, including muscle and nerve [15,26,27]. We implanted a CNT-interfaced PGF neural scaffold in a 10 mm transected sciatic nerve for 16 weeks and the effects on axonal guidance, reinnervation of muscles and the electrophysiological functions were delineated and compared with the findings for a non-interfaced PGF scaffold. It is hoped that this first in vivo study using a CNT-interfaced biomaterial scaffold will provide some informative and pioneering concepts on the possible utility of CNT interfacing as a novel guide and scaffold for the repair and regeneration of nerve tissues.

2. Materials and methods

2.1. Preparation of CNT–PGFs and nerve scaffolds

The composition of phosphate glass was P_2O_5–CaO–Na_2O–Fe_2O_3, with a 50–40–5–5 mol.% ratio. The generation of microfiber bundles of the phosphate glass has been described in detail elsewhere [15]. Produced microfibers were aligned using a microcomb, fixed on one end with heat-melted poly(caprolactone) (PCL; Sigma–Aldrich, St. Louis, MO, USA) solution and then dried. The aligned microfibers were cut to a length and width of about 18 mm, then fixed on the other end with PCL, which can be directly applied in both in vitro and in vivo experiments. Together with the microfiber form, a disc of the phosphate glass was also prepared for characterization of the surface modification of the phosphate glass, after sintering phosphate glass powder of the same composition.

The aligned PGF bundle was interfaced with CNTs, so that it could play the role of a guiding substrate for the neural cells, as depicted in Fig. 1A. The series of chemical reactions for this CNT tethering is shown schematically in Fig. 1B–D. First, the glass surfaces were positively charged with amine residues. The glass microfiber bundles and discs were pretreated with 1 N hydrochloric acid for 5 min, treated with 2.5% 3-aminopropyl-triethoxysilane (APTES; Sigma–Aldrich) at pH 5.0 for 10 s, then dried with a heat gun (~120 °C) 10 times (Fig. 1B). CNT solution was prepared after carboxylation of raw CNTs by the acid oxidation method. Briefly, 0.5 g of CNTs (multi-walled, 15–20 nm outer diameter, 10–20 μm length; EM-Power Co., Asan, Korea) was added to H_2SO_4/HNO_3 1:1 aqueous solution and refluxed at 80 °C for 2 days, followed by filtration through a 0.4 μm Millipore membrane. The resultant carboxylated CNTs were washed and dried under a vacuum, then dissolved in ethanol to a concentration of 0.0025 wt.%. The aminated glass bundles and discs were then soaked in the CNT–COOH solution with 0.006 mM 1-ethyl-3-(3-dimethylaminopropyl) carbodiimide hydrochloride (EDC; Sigma–Aldrich) at room temperature for 3 h to enable amide bonds to form (Fig. 1C). The CNT–PGF surface was further functionalized with amine groups by carbodiimide crosslinking with 0.1 M ethylenediamine (Sigma–Aldrich) and 0.012 mM EDC at pH 5.0 and room temperature for 2 h to leave amine groups at the surface of the CNT–PGF substrate (Fig. 1D). Samples were rinsed with a series of ethanol solutions and distilled water (DW) to remove excess chemical byproducts, before being sterilized first in 70% ethanol and then under UV irradiation for further biological assays.

The aminated CNT–PGF substrate was then incorporated into cylindrical nerve scaffolds. The scaffolding of the microfiber bundles was carried out as a two-step process: first wrapping them around a biopolymer nanofiber mat (Fig. 1E) and then placing it within a porous biopolymer cylindrical tube (Fig. 1F). First, a PLDLA electrospun nanofiber mat was prepared. PLDLA solution in chloroform (2.5 wt.%) was electrospun onto a high-speed rotating metal collector to gather up aligned PLDLA nanofibers. The electrospinning conditions were a 1.5 kV cm^{-1} electric field strength and a 0.1 ml min^{-1} injection speed. The microfiber bundles were placed onto the nanofiber mat, which was then rolled up to wrap (three times) the bundles completely. The number of microfibers wrapped within the nanofiber mat was determined to be 900 ± 36. The nanofiber-wrapped microfiber bundles were then placed within a PLDLA cylindrical tube. The PLDLA tube was produced by the method described elsewhere with a slight modification [28]. In brief, 0.2 g of PLDLA and 1 g of ionic liquid ([bmim]BF_4) were dissolved in 10 ml of dichloromethane, in which a glass tube (0.8 mm diameter) was immersed to coat it with a thin layer (~200 μm) of the PLDLA–ionic liquid. After completely drying, the ionic liquid was selectively dissolved in DW by gentle washing, to leave a porous structured PLDLA cylindrical tube.

2.2. Characterization of CNT–PGFs and scaffolds

The identification and quantitative analysis of chemical reaction were accomplished with a zeta potential analyzer (Zetasizer Nano ZS, Malvern Instruments Ltd., Worcestershire, UK), Fourier transform infrared spectrometry (Varian 640-IR, Varian, Palo Alto, CA, USA), X-ray photoelectron spectroscopy (XPS; AES-XPS ESCA 2000, Thermo Fisher Scientific Inc., Waltham, MA, USA) and thermogravimetric analysis (TGA; TGA N-1500, Scinco, Seoul, Korea). The morphology of the samples was examined by field emission scanning electron microscopy (FESEM; MIRA II LMH microscope, Tescan, Czech Republic) and transmission electron microscopy (TEM; JEM 2000EXII, Jeol Ltd., Tokyo, Japan). The water wetting property of the samples was examined by contact angle analysis (Phoenix 300, Surface Electro Optics, Gyunggido, Korea). The electrical conductivity was analyzed using a high-resistance measurement (Agilent 4339B/4349B, Agilent Technologies, Inc., Santa Clara, CA, USA).

The physical and chemical stability of the CNTs linked to the PGF surface were examined. For the physical stability, microfiber bundles were treated with ultrasound for 10 min, after which the CNTs' existence and status on the surface were observed by FESEM. The chemical stability was observed by soaking the sample in DW for periods of up to 28 days. At predetermined times, the sample was taken out and the surface status was examined by FESEM.

2.3. In vitro study of CNT–PGFs using PC12 and DRG cells

For the in vitro study, aligned microfiber bundles (either PGFs or CNT–PGFs) were used by fixing the ends of bundles with PCL

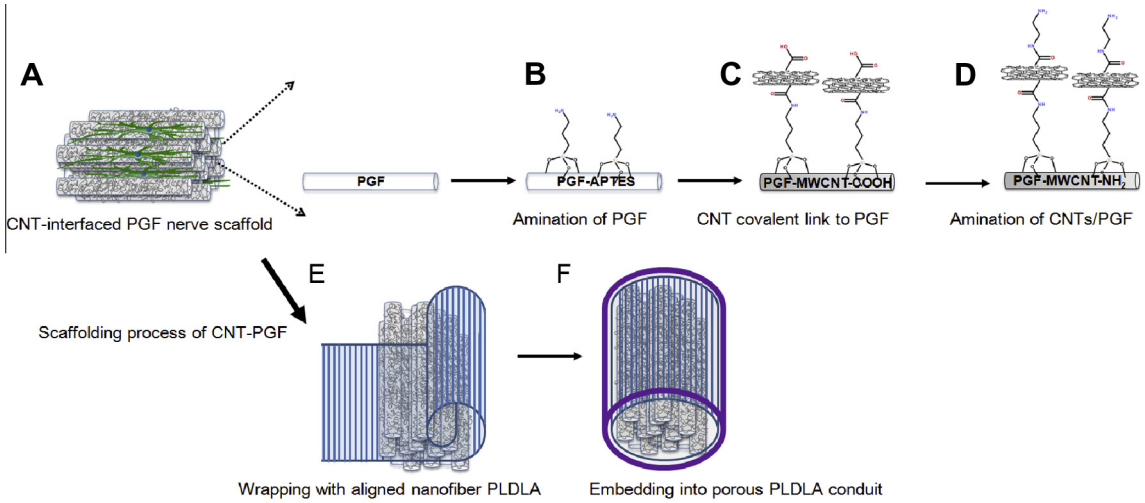

Fig. 1. Schematic presentation of PGFs interfaced with CNTs and a CNT-interfaced PGF scaffold. The aligned PGF bundle interfaced with CNTs for neurite outgrowth (A) was processed from (B) to (D). PGFs were positively charged with amine residues (B), followed by amide bond formation between the primary aminated PGF and the carboxyl groups of the CNT (C), then functionalized with amine groups via the carbodiimide crosslinking reaction (D). For in vivo study, the CNT–PGF substrate was wrapped around a PLDLA electrospun nanofiber mat (E), then placed within a porous PLDLA cylindrical tube (F).

to a length and a width of about 18 mm for a 12-well cell culture system. First, the effects of the any extracts from the CNT–PGF bundles on the cell viability were examined using the PC12 cell line. For this, the microfiber bundles were incubated in the culture medium, which consisted of α-modified Eagle's medium (Welgene Inc., Daegu, Korea), 10% fetal bovine serum (FBS; Gibco®, Life Technologies Inc., Carlsbad, CA, USA), 100 U ml^{-1} penicillin and 100 μg ml^{-1} streptomycin (Gibco®), for either 7 or 14 days at 37 °C. After each period, the extract medium was mixed with the normal culture medium at varying ratios (extract:culture medium = 0:100, 1:99, 10:90 and 30:70) to prepare graded concentrations of the extracts. The PC12 cell line (American Type Culture Collection, Manassas, VA, USA), derived from a pheochromocytoma of the rat adrenal medulla, were grown in normal culture medium at 37 °C in a humidified atmosphere of 5% CO_2. Cells were cultured for 3 days in culture media containing 7 or 14 day dissolved solution. The cell viability was analyzed by means of a Cell Counting Kit-8 (CCK-8; Dojindo Laboratories, Kumamoto, Japan). After reaction for 3 h, the colored formazan product was read at an absorbance 450 nm using a microplate absorbance reader (Bio-Rad Laboratories, Hercules, CA, USA). The test was carried out in triplicate.

Next, we tested the effects of CNTs on the neurite outgrowth of primary neurons using dorsal root ganglion (DRG) cells. Thoracic- and lumbar-spine-level DRG neurons from 6 week old Sprague–Dawley (SD) rats were excised, collected in Hanks' balanced salt solution (Gibco®) and prepared for primary culturing as previously described [15]. CNT–PGFs of approximately 20 mm length were arranged longitudinally on coverslips, both ends attached using liquid PCL and plated onto culture dishes. PGFs without CNTs and coverslips without PGFs were used as a dual control. The coverslips were then coated with 20 μg ml^{-1} poly-D-lysine (Sigma–Aldrich) and 10 μg ml^{-1} laminin (Sigma–Aldrich), and placed in the wells of a 12-well plate.

DRG neurons were mixed in culture medium with 10% FBS (Invitrogen, Life Technologies Inc.) and 1% penicillin/streptomycin, placed in a 37 °C/5% CO_2 incubator and harvested after 4 h. Thus maintained DRG neurons (approximately 3000 cells per well of the 12-well plate) were directly seeded onto each sample (PGFs, CNT–PGFs and culture dish) and then cultured for periods of up to 3 days, with refreshment of medium every 24 h. At each culture period (1, 2 and 3 days), the slides (n = 4 in each group on each day) were fixed with 4% paraformaldehyde in 0.12 M phosphate-buffered saline (PBS) and stained. The primary antibody for axons was mouse SMI312 monoclonal antibody (1:400, Abcam, Cambridge, MA, USA) and the secondary antibody was fluorescein isothiocyanate (FITC)-conjugated goat anti-mouse IgG (1:200, Jackson ImmunoResearch Labs, Inc., West Grove, PA, USA). The stained slides were treated with PBS containing 4′-6-diamidino-2-phenylindole (DAPI) and coverslipped with Vectashield® (Vector Laboratories, Burlingame, CA, USA). For the purposes of a quantitative analysis, the 15 longest SMI312-positive neurites were selected under confocal microscopy. The maximal neurite length was measured using NIH ImageJ software (National Institute of Health, Bethesda, MD, USA) and NeuronJ plugins [29], and averaged according to the groups and periods. Fifteen SMI312-positive DRG neurons in each group and period were randomly selected, and the number of branch points which arose from each neuronal cell body was manually counted and averaged. The number of DRG neurons on each slide was also counted, and a total of three slides per group were used for analysis. All of the measurements were performed by one observer blinded to the group and time period.

2.4. In vivo study in transected rat sciatic nerve model

For the in vivo tests, the CNT–PGF 3-D scaffolds wrapped with PLDLA nanofiber and placed into PLDLA cylindrical tube (as described in Section 2.1) were used. The scaffold dimensions were an inner diameter of 0.8 mm, an outer diameter of 1.0 mm and a length of 12 mm. The CNT-free PGF scaffold, prepared by the same method as the CNT–PGF scaffold, was used as the comparison group.

Adult female SD rats (age: 12 weeks; weight: 230–250 g) were employed, strictly observing all animal care and surgical procedures as approved by the Institutional Animal Care and Use Committee of Dankook University (DKU-11-028). During the experiment, the animals were housed individually at a constant temperature (23–25 °C) and humidity (45–50%) without restriction of food and water. Surgery was performed under isoflurane (Forane, Choongwae Pharma, Seoul, Korea). After the skin and subcutaneous layers around the left hip joint had been incised, the left sciatic nerve was exposed. The sciatic nerve was transected completely from a point 5 mm distal from the left hip joint and removed, leaving a 10 mm gap. Just after injury, both ends of the

transected sciatic nerve were inserted about 1 mm into a 12 mm long PGF or CNT–PGF scaffold, which was then tied to the epineural sheath using 10-0 Nylon. For a positive control, an autologous nerve graft was performed using a 10 mm long transected sciatic nerve following a 180° rotation and reattached with 10-0 Nylon. The muscle, subcutaneous layers and overlying skin were closed with silk. The CNT–PGF- and PGF-implanted rats were sacrificed 16 weeks after implantation. A total of40 rats (14 autologous nerve-grafted rats, 14 CNT–PGF-implanted rats and 12 PGF-implanted rats) were sacrificed throughout the study.

2.5. Immunohistochemistry and histology of sciatic nerves and muscles

For the purposes of a histological analysis, all of the animals were deeply anesthetized, transcardially perfused with saline, and fixed with 4% paraformaldehyde. The injured sciatic nerve was removed, postfixed with 4% paraformaldehyde and immersed for 3 days in 30% sucrose solution. The tissues were embedded in M1 compound (Thermo Fisher Scientific Inc.) and sectioned sagittally or axially on a cryostat at 16 μm. Sections were treated with 0.2% Triton X-100 in 2% BSA/PBS solution and blocked with 10% normal serum. Primary antibodies (mouse SMI312 monoclonal antibody, 1:1000, Covance, Princeton, NJ, USA; rabbit S-100 polyclonal antibody, 1:1000, Dako Cytomation, Carpinteria, CA, USA) were incubated overnight at 4 °C and secondary antibodies (FITC-conjugated goat anti-mouse IgG, 1:200, and Rhodamine-conjugated goat anti-rabbit IgG, 1:200, both from Jackson ImmunoResearch Labs Inc.) were incubated for 2 h at room temperature. Sections were treated with PBS containing DAPI, coverslipped with Vectashield® (Vector Laboratories) and observed by confocal microscopy (Carl Zeiss Inc., Oberkochen, Germany). Whole SMI312-positive axons at the distal stump (1 mm from distal end of scaffold) were counted in the transverse sections; counting was carried out using NIH ImageJ software and combined fully and semi-automated methods were used for nerve morphometry, as described previously [30].

After completion of the electrophysiological evaluation, the gastrocnemius muscles of the injured site were dissected, frozen in liquid-nitrogen-cooled isopentane and cryosectioned at 10 μm. Hematoxylin and eosin (H&E) staining was performed on the gastrocnemius muscles in the autologous-nerve-grafted group and the CNT–PGF and PGF scaffold-implanted groups at 16 weeks (one slide per rat and six rats in each group). Slides were dehydrated, cleared, mounted in DPX (Sigma–Aldrich), and observed under a microscope (Nikon, Tokyo, Japan).

Sections from the belly of the gastrocnemius muscles of the injured site were ATPase stained to determine the muscle fiber type in the autologous-nerve-grafted group and the CNT–PGF and PGF scaffold-implanted groups at 16 weeks (one slide per rat and six rats in each group). The sections were prepared for staining by preincubation in barbital acetate buffer (pH 4.53), followed by incubation in ATP solution. They were then washed with 1% calcium chloride solution, incubated with 2% cobalt chloride and washed in 0.005 M sodium barbital. For visualization, sections were immersed in 2% ammonium sulfide solution followed by rinsing in DW, dehydrated in an ethanol series, cleared with xylene, mounted in DPX and observed under a microscope. Stained muscle sections representing four different rats within the same group were selected for analysis, the cross-sectional area of the gastrocnemius muscle fibers was measured using NIH ImageJ software, and combined fully and semi-automated methods were used for nerve morphometry [30].

2.6. Electrophysiological assessments

Motor nerve conduction studies were performed for all of the experimental and control groups at 16 weeks post-implantation. The animals were anaesthetized with isoflurane (Forane, Choongwae Pharma), and placed on a warmed heating pad. The surrounding adipose and muscle tissues were carefully removed to expose the sciatic nerve. Electrical stimulation was applied by means of electrodes proximal to the nerve graft or scaffold. The stimulation mode was set to pulse (5 mA stimulus intensity, 1 Hz frequency, 1 ms duration); the active surface electrode was placed in the gastrocnemius muscle belly of the injured site, the reference surface electrode near the distal tendon and the ground electrode in the tail. Amplification and recording were accomplished using a data acquisition system (Powerlab 8/35, AD Instruments Inc., Colorado Springs, CO, USA); specifically, the signals were recorded using Labchart 7 software (AD Instruments) connected to a Bio-amplifier (Bioamp, AD Instruments). A notch filter incorporating a band-pass filter set to 1–5000 Hz was utilized to remove 60 Hz of noise from the signals. The peak-to-peak amplitude and onset latency of the compound muscle action potentials (CMAPs) were measured for the autologous-nerve-grafted group and the CNT–PGF and PGF scaffold-implanted groups according to the intensity of stimulation.

2.7. Statistics

Statistical analyses were performed using PASW Statistics 18 (SPSS Inc., Chicago, IL, USA). The Kolmogorov–Smirnov test was conducted to reveal the normal distribution of all quantitative data from the biomaterial properties and the in vitro and in vivo studies. The Kruskal–Wallis test was performed to compare the contact angles of phosphate glass disc (PGD) and functionalized CNT–PGD, the PC12 cell viability cultured in 1%, 10% and 30% PGF and carboxylated or aminated CNT–PGF, and the number of survived DRG neurons cultured on plain dish, PGF and CNT–PGF. Bonferroni correction was also used to pair groups after the Kruskal–Wallis test. One-way analysis of variance (ANOVA) with the Duncan post hoc test was conducted to compare the conductivity measurements of PGD and functionalized CNT–PGD, and the maximal neurite length and branch numbers of DRG neurons cultured on plain dish, PGF and CNT–PGF. The Mann–Whitney *U*-test was performed to compare the quantitative results of axonal and muscle histology and electrophysiology of the PGF and PGF–CNT scaffold-implanted groups. All error bars in figures related to the standard error of the mean, and statistical significance was set at $p < 0.05$.

3. Results

3.1. Fabrication of CNT–PGF nerve scaffolds

The CNTs used in this study were carboxylated by acid treatment and their properties are presented as Supplementary data (Fig. S1). Unlike raw CNTs, which are not readily soluble in ethanol, the carboxylated-CNTs showed excellent solubility, with the solvent stability lasting for months (Fig. S1A). Zeta-potential measurements revealed a highly negatively charged surface (−43 mV), which was explained by the presence of a large number of carboxylic groups (Fig. S1B). Fourier transform infrared spectroscopy confirmed the development of carboxylic groups in the acid-treated CNTs (Fig. S1C) and the XPS results showed a higher oxygen peak related to the carboxylic group (Fig. S1D). TGA showed a difference in thermal degradation behavior between the two groups, with more weight loss in the carboxylated CNTs, suggesting that thermal weight loss occurred in the carboxylic groups (Fig. S1E). A TEM image of the CNTs showed that acid treatment decreased the wall thickness of the CNTs slightly (Fig. S1F). The results clearly show that the multi-walled CNTs used in this study were carboxylated well and highly negatively charged.

Using the carboxylated CNTs, the surface of the PGFs was changed through a series of chemical reactions, and the CNT–PGF bundles were then developed into 3-D nerve scaffolds (as illustrated in Fig. 1). Fig. 2 shows scanning electron microscopy (SEM) images of the samples (CNT–PGF and 3-D scaffold) during the process. After the melt-spinning of glass powder, PGFs were easily generated aligned in a single direction and were very uniform in size (Fig. 2A). The average size of the PGFs ($n = 100$), as analyzed by SEM and calculated by the ImageJ image analysis program, was 22.32 ± 3.73 μm (range: 12.17–29.00 μm). This is within the optimal range for neuronal cell attachment and culturing on our phosphate glass poles, given that the reported diameters of the neuronal cell bodies are 5–20 and 5–50 μm for PC12 cells and DRG neuronal cells, respectively [31,32]. We optimized the conditions for the tethering of carboxylated CNTs on PGF bundles by varying the concentration and frequencies of APTES treatment and the concentration of the CNT solution. A homogeneous monolayer-coated surface could be achieved on the CNTs on the PGFs (Fig. 2B) by first using a low-concentration APTES solution while enabling the PGF-amination reaction to occur three times, then by using a diluted and better-dispersed CNT solution while enabling the amide reaction to occur five times. A highly non-homogeneous CNT coating is achieved when using a thick CNT solution (Fig. 2C), and this also happens when the APTES treatment is not properly carried out. The CNT-interfaced PGFs were subsequently aminated via the carbodiimide reaction using a diamine solution. The amination process was confirmed to preserve the morphology of the CNTs interfaced with the PGFs well. Next, the CNT–PGF bundles were constructed into a 3-D scaffold, first by rolling onto a PLDLA aligned nanofiber and then placing it within a PLDLA microporous tubular conduit. The morphology of the 3-D nerve scaffold containing the microfibers depicted in Fig. 2D shows the functional arrangement of each component, i.e. the microfibers packed inside, the thin wrapping sheet and the slightly thicker outermost layer. A higher magnification of the inner thin sheet revealed the nanofibrous morphology aligned parallel to the microfibers (Fig. 2E). Also, the outer shell presented a highly microporous with pore sizes of 50–100 mm (Fig. 2F).

3.2. Physicochemical properties of the CNT–PGF

The physicochemical properties of samples underwent each chemical modification step were then in-depth analyzed. The chemical analyses were particularly carried out using a disc type of the same phosphate glass composition. First, the XPS signals showed energy peaks of atoms present on the outermost surface (Fig. 3A). The chemical shift from 284.63 to 285.07 eV, for a difference of 0.17–0.44 eV in the carbon atom binding energy of the C1s, is associated with CNT modification, in contrast to CNT-free glass substrate. The XPS spectra of the CNT-modified phosphate glass reflected the highest carbon atom (74.90%) and oxygen atom (18.39%) contents. It was obvious that this was due to the sp^2 carbon atoms of the CNT molecules covalently bound to the glass. The amination of CNT-glass showed an increased percentage of nitrogen (5.68%). This suggests that the open-end structures of the CNT molecules and the functional groups bonded to the nanotubes' end loops on the discs. Fig. 3B demonstrates the surface wettability changed according to the surface chemistry. The phosphate glass (PGD) showed the highest hydrophilicity due to a bunch of ionic groups on the surface, whereas the APTES-treated glass (PGD-APTES) became hydrophobic due to the creation of silane groups. The CNT-tethering increased the hydrophilicity (PGD-MWCNT-COOH) and the subsequent amination (PGD-MWCNT-NH_2) increased further ($p < 0.05$ by Kruskal–Wallis test). As one of the distinct advantages of CNTs-interfacing is the electrical conductivity, we calculated the value by measuring the resistance of each sample, as shown in Fig. 3C. The conductivity of CNT-free phosphate glass (PGD) and APTES-treated glass (PGD-APTES) samples ranged approximately 10^{-13} S cm^{-1}, like insulators. However, the CNTs interfacing substantially increased the conductivity level to approximately 10^{-5}–10^{-6} S cm^{-1}, and the post-amination also showed a similar level.

Next, the stability of CNTs tethered onto PGF was examined by means of either ultrasound sonication for 10 min or soaking in water for up to 28 days, as shown in Fig. 4. The SEM morphology of microfibers after 10 min of ultrasonic treatment showed little change in the CNT layered morphology from that before sonication.

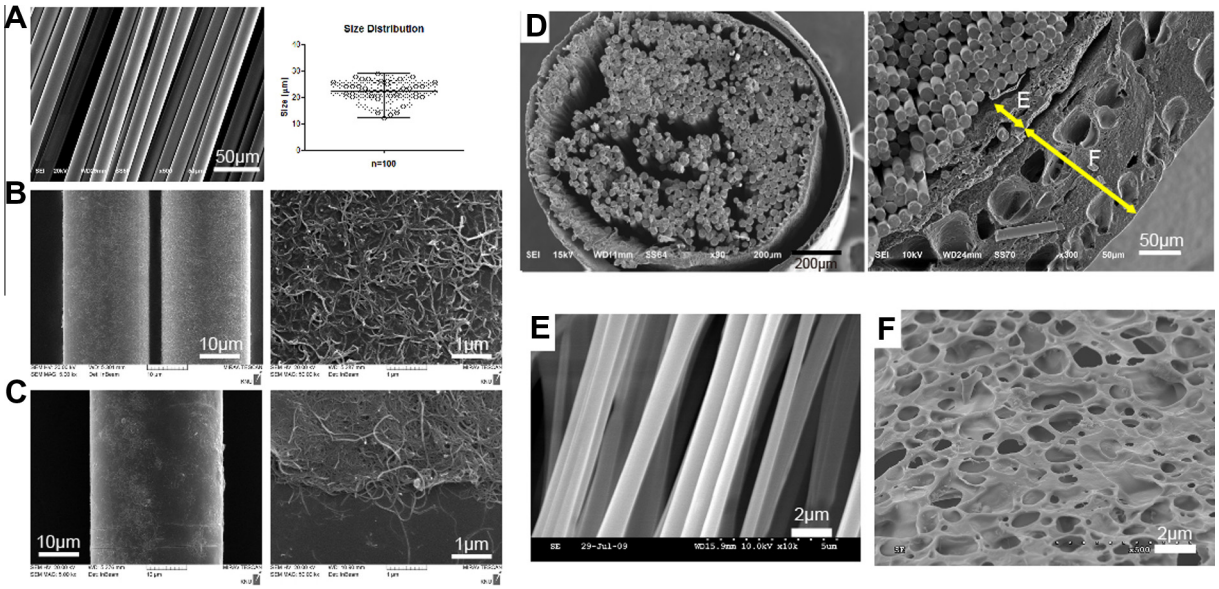

Fig. 2. SEM morphology analysis of CNT-interfaced PGFs (CNT–PGFs) and a scaffold for in vivo study. Uniformly aligned PGFs (A, left) and the distribution of the diameter of randomly selected 100 PGFs (A, right). Optimized CNT–PGFs showed a homogeneous monolayer-coated surface (B), and a non-homogeneous CNT coating was achieved when thick CNT solution was used (C). (D–F) SEM image showing the structure of a 3-D CNT-interfaced PGF scaffold: (D) the whole cross-sectional structure (left), with magnified images of the periphery of the scaffold (right); (E) magnified surface (aligned fiber structure) of inner PLDLA mat; and (F) magnified surface (porous structure) of the outer PLDLA tube.

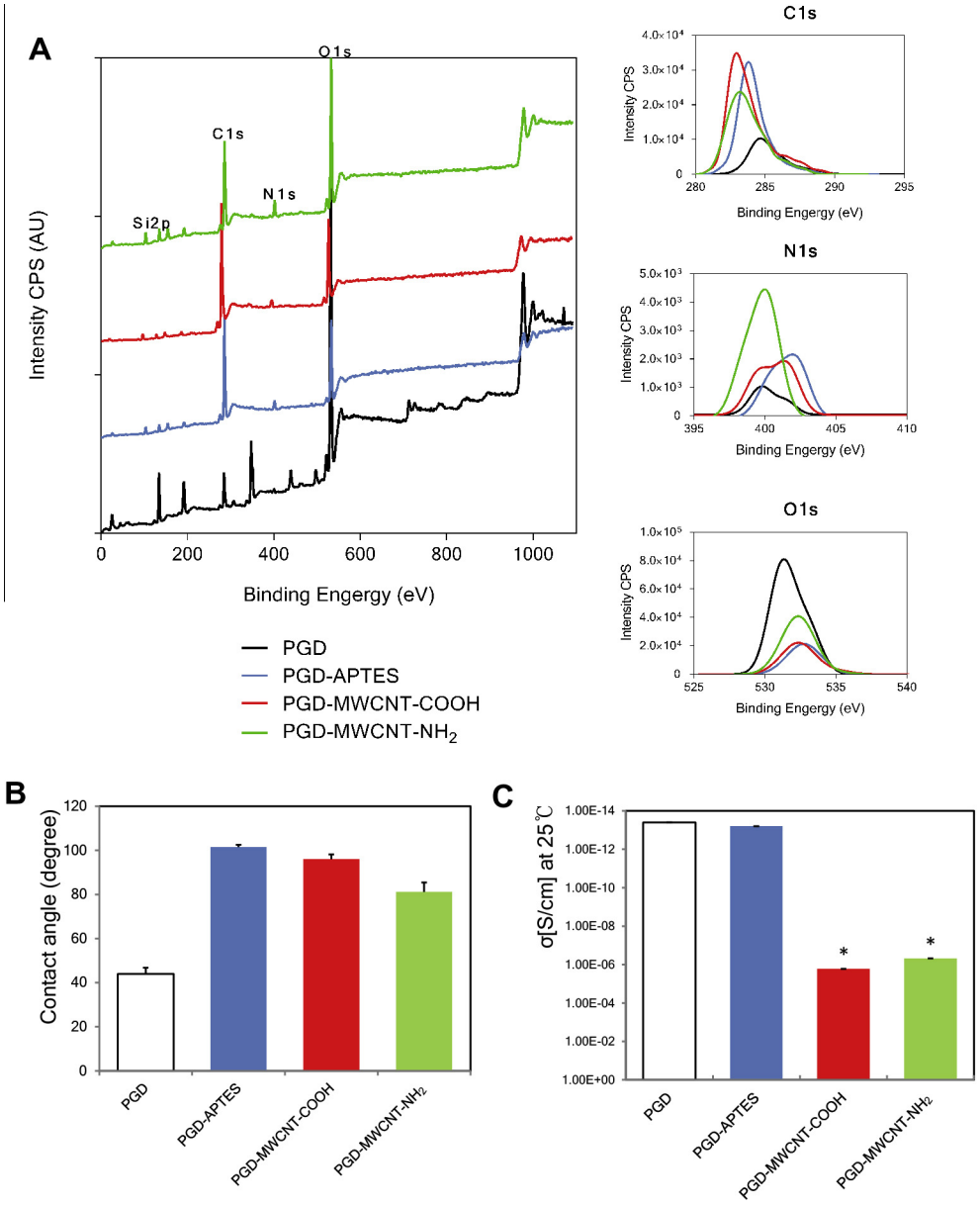

Fig. 3. Chemical properties of PGD, APTES-treated PGD (PGD–APTES) and CNT-interfaced PGD with carboxylation (PGD–MWCNT–COOH) or amination (PGD–MWCNT–NH_2). (A) XPS analysis of surfaces of PGD or CNT-interfaced discs. (B) Contact angle and (C) conductivity measurement of samples. *$p < 0.05$ compared with PGD by the Kruskal–Wallis test with Bonferroni correction. The error bar relates to the standard error of the mean.

Moreover, the SEM image of microfibers during water immersion at varying period evidenced the CNTs were soundly present on the glass surface with a similar morphology to that before water immersion. Interestingly PGFs did not show any significant surface erosion and thus resultant CNTs detachment.

3.3. In vitro study of CNT–PGFs in PC12 and DRG cells

PC12 cells were cultured for 3 days in culture media containing 7-day or 14-day PGF or CNT–PGF dissolved solution with different concentration. According to the results, PGF or CNT–PGF dissolved solution showed no cytotoxicity, and PC12 cells even showed better cell viability in the carboxylated or aminated CNT-interfaced PGF soaking solution than in any of the PGF dilutions. PC12 cell viability was significantly improved as the dilution percentage increased from 1% to 30% in 7-day dissolved solution (Fig. 5A), and also had a tendency to be increased with the concentration in 14-day dissolved solution (Fig. 5B).

Based on this cellular toxicity study, we next assessed neurite outgrowth behaviors of primary neurons on the CNT–PGFs. Primary cultured DRGs extracted from 6-week-old SD rats were placed either on CNT–PGFs, on PGFs without CNTs, or in a plain dish, and cultured for 3 days. Whilst neurites outgrew randomly in the control dish, neurites extended directionally on the microfiber substrates, and the extension was much higher on the CNT–PGFs than on the PGFs (Fig. 5C). Analyses of the neurite outgrowth gave significant difference between groups. The maximal neurite length was significantly higher on the CNT–PGFs than on the PGFs or those cultured in the plain dish (Fig. 5D); further, the branch numbers per DRG did not differ between the CNT–PGFs and the PGFs (Fig. 5E), and the number of attached DRGs at 3 days was greater on the CNT–PGFs than on the PGFs (Fig. 5F).

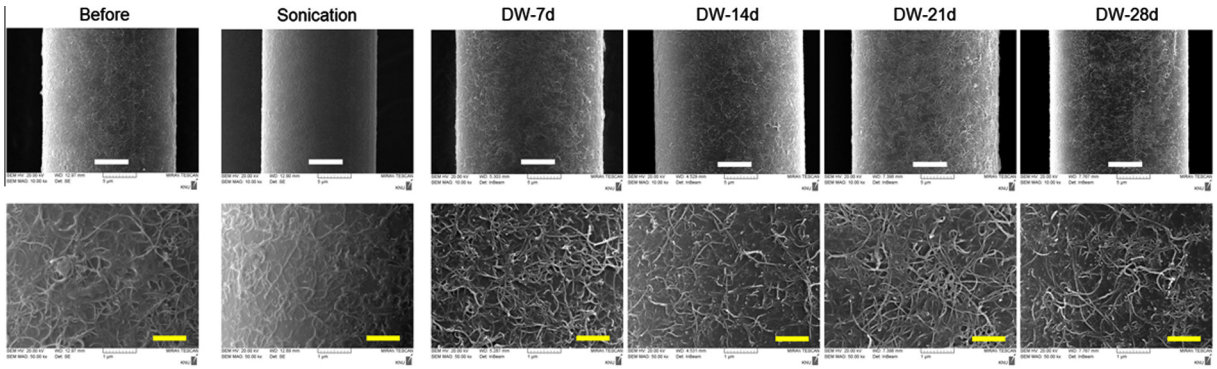

Fig. 4. Stability of the CNTs interfaced onto the PGFs as observed by SEM. CNT-interfaced images with different treatments shown for comparison: before (as-prepared) and after ultrasonic treatment for 10 min, and after soaking in distilled water (DW) for up to 28 days (7, 14, 21 and 28 days at low (top, white scale bar = 5 μm) and high magnification (bottom, yellow scale bar = 1 μm).

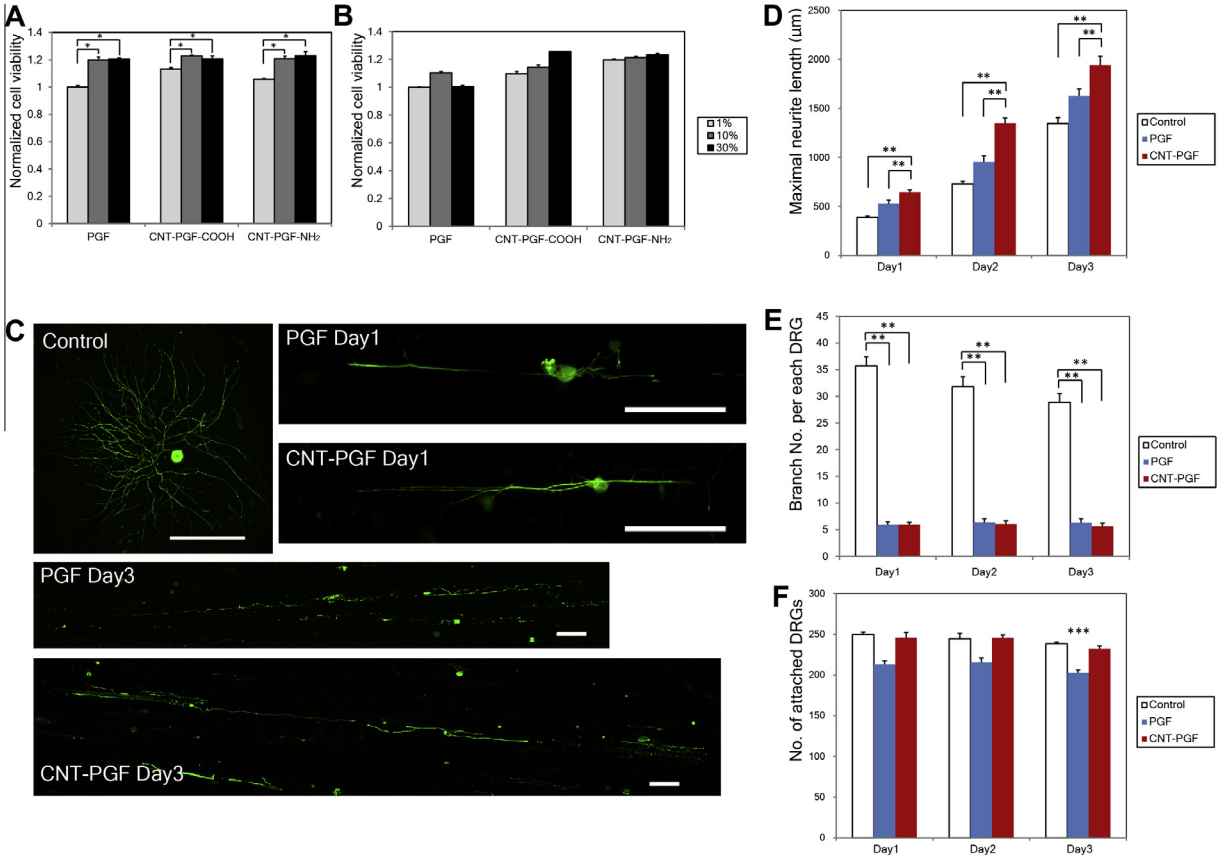

Fig. 5. Cell viability assay with PC12 cells in culture media mixed with various concentrations of PGF or functionalized (carboxylated (COOH) or aminated (NH_2)) CNT–PGF solutions dissolved for 7 (A) and 14 days (B). (C) Representative images of DRG neuronal cell culture on plain dish (Control), PGFs or optimally functionalized MWCNT-interfaced PGFs (CNT–PGF) for 1 and 3 days. Quantitative results of the maximal length of DRG neuritis (D), number of branches per DRG (E) and numbers of attached and surviving DRGs (F) of each group (plain dish, PGFs and CNT–PGFs). Scale bar = 200 μm. $^{*}p < 0.05$ by the Kruskal–Wallis test with Bonferroni correction; $^{**}p < 0.05$ by one-way ANOVA with the Duncan post hoc test; $^{***}p < 0.05$ by the Kruskal–Wallis test. The error bar relates to the standard error of the mean.

3.4. In vivo study of CNT–PGFs in peripheral nerve injury

The produced 3-D scaffolds (CNT–PGFs and CNT-free PGFs) were implanted into transected stumps to fill a 10 mm gap after complete transection of the sciatic nerve of 12-week-old SD rats (Fig. 6A). We found that SMI312-positive axons crossing the implanted scaffold and S100-positive Schwann cells along the axons was more in CNT–PGF group than in PGF group (Fig. S2A and B) and the number of SMI312-positive axons at the distal stump of the CNT–PGF group was significantly higher than that in the PGF group (Figs. 6B, C and 7A). The cross-sectional area of the gastrocnemius muscle was significantly larger in the CNT–PGF group than in the PGF group (Figs. 6D and 7B). Following CNT–PGF scaffold implantation, the mean value of the proportion of the type I fiber of the gastrocnemius muscle was decreased and that of the type IIa fiber was increased, more so than with the PGF scaffold (Figs. 6E and 7C), but without statistical difference. The onset to the peak amplitude of the CMAPs in gastrocnemius muscle also was larger in the CNT–PGF group than in the PGF group (Figs. 6F and 7D).

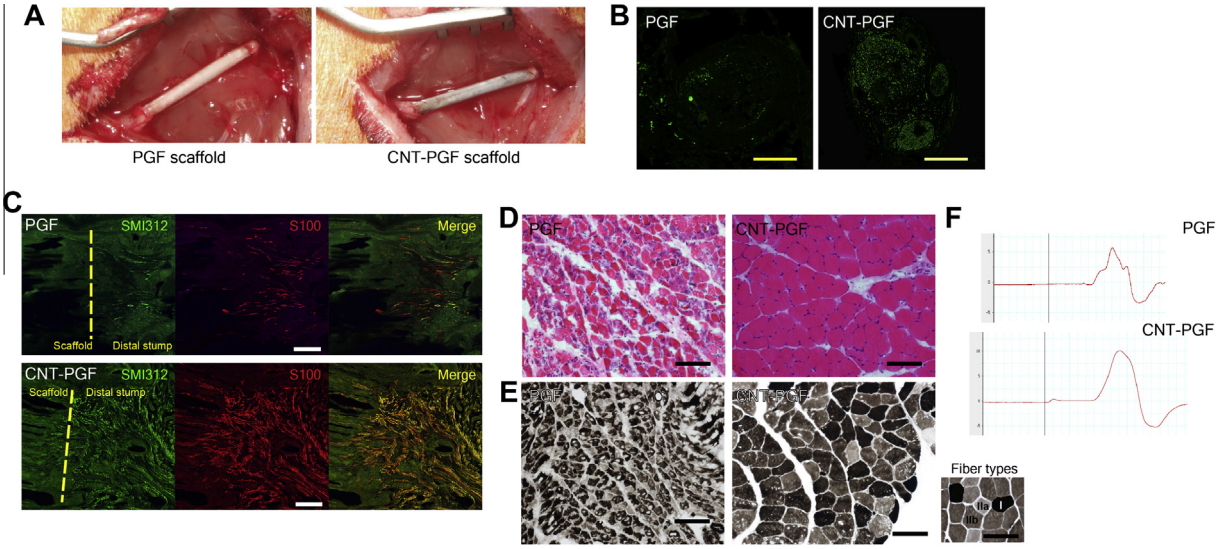

Fig. 6. In vivo experiments and findings of functionalized CNT-interfaced PGF scaffolds. (A) Implantation of CNT-free PGF (PGF) or CNT-interfaced PGF (CNT–PGF) scaffold between the proximal and distal stumps of a completely transected rat sciatic nerve. Representative immunohistochemical images of axons (green) in the transverse section at the distal stump (11 mm from the proximal stump end, B) and axons (SMI312, green), and Schwann cells (S100, red) in the sagittal section at the border between the scaffold and the distal stump (C) of PGF scaffold-implanted sciatic nerve (PGF) or CNT–PGF scaffold-implanted sciatic nerve (CNT–PGF) at 16 weeks post-implantation (yellow scale bar = 500 μm, white scale bar = 200 μm). (D) Representative images of H&E-stained gastrocnemius muscle following PGF scaffold (PGF) or CNT–PGF scaffold implantation (CNT–PGF) at 16 weeks post-implantation (black scale bar = 50 μm). (E) Representative images of ATPase stained muscle (PGF and CNT–PGF) and examples of muscle fiber types (right, I = type I, Iia = type IIa, Iib = type IIb, black scale bar = 50 μm). (F) Representative images of CMAP following PGF scaffold (PGF) or CNT–PGF scaffold implantation (CNT–PGF).

4. Discussion

In this study, we demonstrated for the first time the in vivo functions of CNT-interfaced implants for the nerve regeneration in rat sciatic model. For this, we designed a novel CNT-tethered nerve conduit based on the phosphate glass microfibers combined with polymeric scaffolds. In particular, CNTs linked to a phosphate glass fiber were functionalized by a series of reactions involving carboxylation and subsequent amination, and the amination was aimed to provide the outermost CNTs surface with amino groups that are considered a more favorable surface, at least when compared with carboxylated surface, for neuronal cell behaviors including cell adhesion, neuronal differentiation of neural stem cells, and in vivo recovery after ischemic stroke [16,22,23,33]. Among other surface properties that may be impacted by the CNT modification, including increased (nano) roughness, altered chemistry, and hardness, the conductivity is believed to be the most fascinating aspect of the conduits for neural applications. In fact, whilst free phosphate glass samples showed a conductivity value of $\sim 10^{-13}$ S cm^{-1}, like insulators, the CNT-interfaced samples substantially increased the conductivity to a range of $\sim 10^{-5}$–10^{-6} S cm^{-1}. This apparent result suggests that the monolayer coverage of CNTs provides the phosphate glass substrate more electrically conductive surface that possibly alters and even stimulates neuronal cell responses.

We subsequently 3-D structured the CNTs-interface phosphate glass fiber for implantable nerve conduit by bundling the CNTs-phosphate glass fibers, followed by wrapping onto a PLDLA nanofiber and then embedding within a porous PLDLA tube. Consequently, the CNTs-glass fibers were stably positioned within a tubular structure, where the porous tubes are freely to interact with outer environments, beneficial for mass transport and blood circulation, which enabling the CNTs-glass fibers to function neural guidance effectively. In fact, when free-CNTs (not tethered onto a substrate) were directly treated to neural cells, many studies have reported their cytotoxicity and genotoxicity [34–38]. Therefore, the surface-tethered CNTs are considered to be much safer as they avoid rapid and direct cellular internalization while providing electrical stimuli to cells in the intercellular and/or cell-matrix interfacing reactions. As to the stability of CNTs onto the phosphate glass fiber, we confirmed the currently implemented CNTs, covalently linked to a phosphate glass substrate, showed to be very stable physically and chemically as they did not dissolve out from the surface to the in vitro test period (for a month). Furthermore, in vivo findings did not reveal any toxic responses related with the CNTs. Phosphate-based glass is usually soluble, but in this study, we used P_2O_5–CaO–Na_2O–Fe_2O_3 with the smallest sodium (5%) and the highest iron (5%) composition which has the least solubility. This fact alleviates any possible concerns on the premature release of CNTs and resultant cytotoxicity, rather, allows for anticipating the CNT–PGF system as a biocompatible nerve guiding matrix.

The CNTs-interfaced phosphate glass fiber scaffolds showed good viability of PC12 cells in the indirect dilution study (Fig. 5A and B). In particular, the improved PC12 cell viability with the diluents demonstrated the possible role of ionic extracts from the glass fibers played in stimulating cell metabolism. In fact, the phosphate glass fiber composition used herein has previously shown to release sufficient amount of ions such as calcium and phosphate that is favorable for cell viability and blood vessel formation [39,40].

Schwann cell is important to support axonal outgrowth and remyelination, and CNTs may affect the survival and proliferation of Schwann cells following peripheral nerve injury [41–43]. In previous in vitro studies, single-walled CNTs in three dimensional hydrogel has no toxicity on Schwann cells [41], and multi-walled CNT containing collagen/PCL fibers might support Schwann cell adhesion [42]. In vivo condition, single-walled CNTs-based silk/fibronectin nerve conduits enhanced S-100 expression of Schwann cells [43]. We found that Schwann cells along CNT-interfaced PGFs were more than those on CNT-free PGFs in vivo study, but we need to delineate the exact mechanisms of CNT-interfacing on the survival and proliferation of Schwann cells in the further study.

With regard to this ionic role on nerve cells, more in-depth studies will be needed in the future, which is considered an interesting

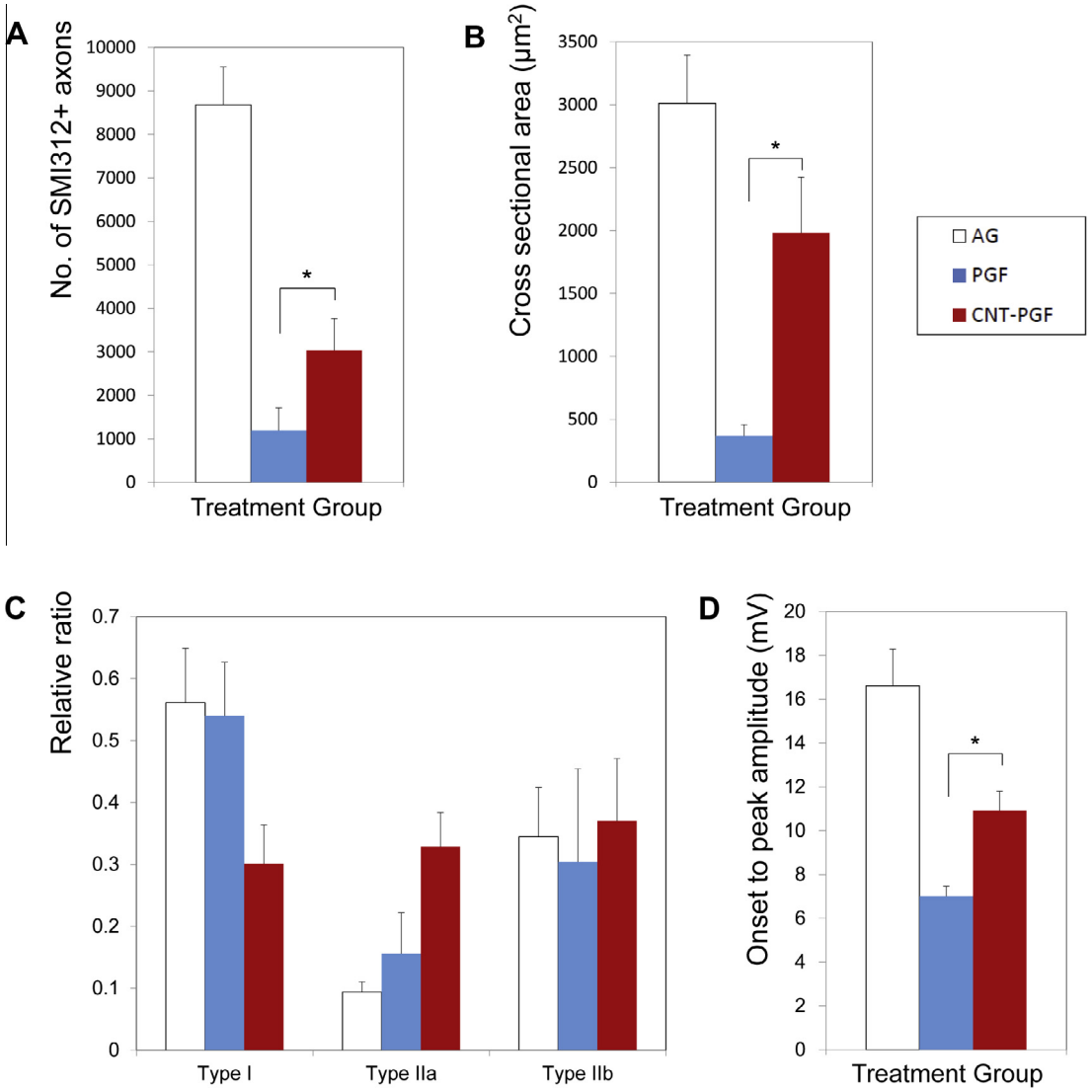

Fig. 7. Quantitative analyses of axonal and muscle histology and electrophysiology. (A) The number of SMI312-positive axons from the cross-sections at the distal stump (11 mm from proximal stump end) and (B) the mean cross-sectional area of gastrocnemius muscle fibers in the autologous nerve graft control and the PGF and PGF–CNT scaffold-implanted groups. (C) The ratio of each muscle type (types I, IIa and IIb; bottom right) following autologous nerve graft control and PGF and CNT–PGF scaffold-implanted groups. (D) The mean values of the onset to peak amplitude in the autologous nerve graft and the PGF and PGF–CNT scaffold-implanted groups (bottom). $^{*}p < 0.05$ between PGF and CNT–PGF scaffold-implanted groups by the Mann–Whitney *U*-test. The error bar relates to the standard error of the mean.

area of study to develop novel scaffolds for neural regeneration As discussed, the ionic release would be possible from the phosphate glass fiber over a long period, which however, is not considered to be an enough level to result in the dissolution of CNTs from the surface. Thus the CNT-interfaced outermost of the phosphate glass fiber implant would be stable at least to the test period, facilitating beneficial cellular interactions. In fact, in the direct culture of DRG cells, the glass fibers demonstrated nerve guidance role, with significant decrease in the neurite branches. Previously, we also found that DRG neurites grew actively along PGFs, which provided physical guidance and offered excellent cellular compatibility [15]. More than this guidance role, the CNT-interfaced on the glass fiber significantly enhanced the cell adhesion level and neurite outgrowth length. The exact mechanism of the effect of CNTs on neuronal growth is yet to be disclosed [24]. It is first thought that the CNTs provided a nanotopological cue to improve the neuronal cell adhesion. CNTs-substrate has been shown to stimulate cell adhesion related gene expression in vitro and the subsequent cell proliferation [44]. Some researchers have suggested that CNTs activate extracellular signal-regulated kinase (ERK) signaling and phospholipase C signaling pathways [33,45]. The high electrical conductivity of CNTs might also affect the neuronal regeneration through the modification of ionic transport across the plasma membrane, by which the ECM protein conformation and synthesis is changed [46], and the neurotrophic factor release from neuronal cells is stimulated [47]. Therefore, the integration of CNTs with the phosphate glass fiber is thought to have a synergistic effect on the DRG functions in terms of providing physical guidance as well as stimulating cell adhesion and neurite outgrowth. The physical, chemical, topological and electrical properties provided by the CNTs-phosphate glass are thus considered promising cues for neuronal functions and possible nerve regeneration.

We demonstrated for the first time the in vivo performance of the CNT-interfaced scaffolds using a completely transected peripheral nerve injury model in rats. While most studies on CNT-based substrates have focused on the in vitro cell behaviors, little is known about the in vivo functions of CNT scaffolds. In fact, only a few recent studies have reported striking findings on the effective

roles of CNTs in the in vivo central nervous systems including brain stroke and spinal cord injury models [16,17]. Aminated CNTs-solution directly injected to a rat brain in stroke model significantly enhanced neural protection and functional restoration [16]. CNTs functionalized with polyethylene glycol, directly injected to the injured spinal cord of rat, effectively reduced lesion volume, increased the number of neurofilaments and functional restoration [17]. These pioneering in vivo studies on CNTs, however, showed the function of CNTs added directly to the injured sites in solution form, instead of reporting the role of CNTs as scaffolds or substrates. Therefore, this study is, to the best of our knowledge, is the first in vivo finding of the performance of CNT-based scaffolds. Here we tested the function of CNTs-interfaced glass fiber in the peripheral nerve injury model, which is considered common clinically encountered injury, thus requiring significant clinical needs, and the outcome can also be applied in parallel to the central nervous system in the future study. In previous studies, the scaffolds containing aligned or structured intraluminal guidance enhanced peripheral and central nerve regeneration [48–50]; we also observed the role of phosphate glass fiber in physically guiding the nerve regeneration. More than this, we found some clear evidences that the CNTs-interfacing functioned better as the intraluminal structured nerve conduit. The number of lesion-crossing axons was significantly increased by the CNTs-interfacing. In fact, phosphate glass fiber conduits inside a collagen scaffold have also shown very limited effect on intraluminal structure during the early stage of up to 8 weeks, with no further functional restoration at 12 weeks [15]. The CNT-interfaced phosphate glass fiber scaffold, however, prolonged the effects of axonal regeneration up to 16 weeks. CNTs can also play roles in drug delivery systems and stem cell differentiation. A CNT-mediated drug delivery system was shown to effectively transport siRNA or other proteins to the target tissue and to achieve functional restoration following brain lesion [51], and, in combination with stem cell transplantation, also improved functional recovery and enhanced stem cell differentiation [52].

Furthermore, we found that the CNT-interfaced PGF scaffold was effective in restoring motor functions electrophysiologically. Motor nerve conduction study showed that CMAP was significantly higher at the CNT interface. This indicates that scaffold-crossing axons were successfully reinnervated into the gastrocnemius muscles and that the muscle was functionally improved as a result of the CNT interfacing. The proportion of slow to fast muscle fiber types usually changes following denervation and reinnervation, with more fast fibers [53], and we found that this tendency was enhanced in rats receiving a CNT-interfaced scaffold. However, there was no clear evidence of any change in the muscle fiber types of reinnervated gastrocnemius muscles following complete transection of the sciatic nerve, and this result was not statistically different from those rats receiving the PGF scaffold or those receiving autologous nerve.

Although we clearly observed the effectiveness of CNT interfacing in peripheral nerve regeneration, the phosphate glass fiber conduit used herein is not considered to provide any better conditions to those in the autologous nerve graft, as deduced from the series of in vivo results. This is due primarily to the limitations of the morphological and physicochemical properties of the phosphate glass fiber bundles. Firstly, although the phosphate glass fibers were developed to have an average diameter of 20–30 μm, the interspacing between the fibers appeared to be somewhat smaller than the optimal spacing for neuronal growth. Secondly, the elasticity of the glass fibers was intrinsically higher than the much softer nerve tissues, and this may not provide the best conditions for neuronal development. To this end, further study will be needed to develop nerve conduits with better morphological and elastic properties, with which the effects of CNTs-interfacing are envisaged to be synergized. Furthermore, as the CNTs interfaced at the edges of the nerve conduit have the potential to carry therapeutic molecules [54,55], including neurotrophic factors and neuroprotective/anti-inflammatory drugs, combining this drug delivery strategy with the CNT-based nerve conduits should improve the capacity to regenerate nerve tissues, possibly to the status of an autologous nerve graft.

5. Conclusions

Carbon nanotubes were successfully interfaced on phosphate glass fibers for nerve guidance and then implemented into a 3-D scaffold which possessed physicochemical integrity with good cell viability and neuronal interactions. These first in vivo findings of carbon nanotube-interfaced nerve implants assessed in a rat sciatic injury model demonstrate the effective roles of the carbon nanotubes in the nerve regeneration process. This study is believed to open up a new class of neural scaffolds based on a electrically conductive nanomaterial – carbon nanotubes.

Disclosure

No potential conflict of interest relevant to this article was reported.

Acknowledgements

This research was supported by a grant of the Korea Health Technology R&D Project (HI14C0522) through the Korea Health Industry Development Institute (KHIDI), funded by the Ministry of Health & Welfare, and the Priority Research Centers Program (2009-0093829) through the National Research Foundation (NRF) funded by the Korean Ministry of Education, Science, and Technology, Republic of Korea.

Appendix A. Figures with essential colour discrimination

Certain figures in this article, particularly Figs. 1–7 are difficult to interpret in black and white. The full colour images can be found in the on-line version, at http://dx.doi.org/10.1016/j.actbio.2014.11.026.

Appendix B. Supplementary data

Supplementary data associated with this article can be found, in the online version, at http://dx.doi.org/10.1016/j.actbio.2014.11.026.

References

[1] Chan KM, Gordon T, Zochodne DW, Power HA. Improving peripheral nerve regeneration: from molecular mechanisms to potential therapeutic targets. Exp Neurol 2014;261C:826–35.
[2] Lee SK, Wolfe SW. Peripheral nerve injury and repair. J Am Acad Orthop Surg 2000;8:243–52.
[3] Meek MF, van der Werff JF, Klok F, Robinson PH, Nicolai JP, Gramsbergen A. Functional nerve recovery after bridging a 15 mm gap in rat sciatic nerve with a biodegradable nerve guide. Scand J Plast Reconstr Surg Hand Surg 2003;37:258–65.
[4] Stoyanova II, van Wezel RJ, Rutten WL. In vivo testing of a 3D bifurcating microchannel scaffold inducing separation of regenerating axon bundles in peripheral nerves. J Neural Eng 2013;10:066018.
[5] Xie J, MacEwan MR, Liu W, Jesuraj N, Li X, Hunter D, et al. Nerve guidance conduits based on double-layered scaffolds of electrospun nanofibers for repairing the peripheral nervous system. ACS Appl Mater Interfaces 2014;6:9472–80.
[6] Ouyang Y, Huang C, Zhu Y, Fan C, Ke Q. Fabrication of seamless electrospun collagen/PLGA conduits whose walls comprise highly longitudinal aligned nanofibers for nerve regeneration. J Biomed Nanotechnol 2013;9:931–43.

[7] Ramburrun P, Kumar P, Choonara YE, Bijukumar D, du Toit LC, Pillay V. A review of bioactive release from nerve conduits as a neurotherapeutic strategy for neuronal growth in peripheral nerve injury. Biomed Res Int 2014;2014:132350.
[8] Chung TW, Yang MC, Tseng CC, Sheu SH, Wang SS, Huang YY, et al. Promoting regeneration of peripheral nerves in vivo using new PCL-NGF/Tirofiban nerve conduits. Biomaterials 2011;32:734–43.
[9] Hsu SH, Kuo WC, Chen YT, Yen CT, Chen YF, Chen KS, et al. New nerve regeneration strategy combining laminin-coated chitosan conduits and stem cell therapy. Acta Biomater 2013;9:6606–15.
[10] Murray-Dunning C, McArthur SL, Sun T, McKean R, Ryan AJ, Haycock JW. Three-dimensional alignment of schwann cells using hydrolysable microfiber scaffolds: strategies for peripheral nerve repair. Methods Mol Biol 2011;695:155–66.
[11] Gu X, Ding F, Williams DF. Neural tissue engineering options for peripheral nerve regeneration. Biomaterials 2014;35:6143–56.
[12] Bell JH, Haycock JW. Next generation nerve guides: materials, fabrication, growth factors, and cell delivery. Tissue Eng Part B Rev 2012;18:116–28.
[13] Cao J, Sun C, Zhao H, Xiao Z, Chen B, Gao J, et al. The use of laminin modified linear ordered collagen scaffolds loaded with laminin-binding ciliary neurotrophic factor for sciatic nerve regeneration in rats. Biomaterials 2011;32:3939–48.
[14] Dornseifer U, Fichter AM, Leichtle S, Wilson A, Rupp A, Rodenacker K, et al. Peripheral nerve reconstruction with collagen tubes filled with denatured autologous muscle tissue in the rat model. Microsurgery 2011;31:632–41.
[15] Kim YP, Lee GS, Kim JW, Kim MS, Ahn HS, Lim JY, et al. Phosphate glass fibres promote neurite outgrowth and early regeneration in a peripheral nerve injury model. J Tissue Eng Regen Med 2012.
[16] Lee HJ, Park J, Yoon OJ, Kim HW, Lee do Y, Kim do H, et al. Amine-modified single-walled carbon nanotubes protect neurons from injury in a rat stroke model. Nat Nanotechnol 2011;6:121–5.
[17] Roman JA, Niedzielko TL, Haddon RC, Parpura V, Floyd CL. Single-walled carbon nanotubes chemically functionalized with polyethylene glycol promote tissue repair in a rat model of spinal cord injury. J Neurotrauma 2011;28:2349–62.
[18] Mattson MP, Haddon RC, Rao AM. Molecular functionalization of carbon nanotubes and use as substrates for neuronal growth. J Mol Neurosci 2000;14:175–82.
[19] Lee JH, Lee JY, Yang SH, Lee EJ, Kim HW. Carbon nanotube–collagen three-dimensional culture of mesenchymal stem cells promotes expression of neural phenotypes and secretion of neurotrophic factors. Acta Biomater 2014;10:4425–36.
[20] Fabbro A, Bosi S, Ballerini L, Prato M. Carbon nanotubes: artificial nanomaterials to engineer single neurons and neuronal networks. ACS Chem Neurosci 2012;3:611–8.
[21] Jin GZ, Kim M, Shin US, Kim HW. Neurite outgrowth of dorsal root ganglia neurons is enhanced on aligned nanofibrous biopolymer scaffold with carbon nanotube coating. Neurosci Lett 2011;501:10–4.
[22] Huang YJ, Wu HC, Tai NH, Wang TW. Carbon nanotube rope with electrical stimulation promotes the differentiation and maturity of neural stem cells. Small 2012;8:2869–77.
[23] Landers J, Turner JT, Heden G, Carlson AL, Bennett NK, Moghe PV, et al. Carbon nanotube composites as multifunctional substrates for in situ actuation of differentiation of human neural stem cells. Adv Healthc Mater 2014.
[24] Fabbro A, Villari A, Laishram J, Scaini D, Toma FM, Turco A, et al. Spinal cord explants use carbon nanotube interfaces to enhance neurite outgrowth and to fortify synaptic inputs. ACS Nano 2012;6:2041–55.
[25] Fabbro A, Prato M, Ballerini L. Carbon nanotubes in neuroregeneration and repair. Adv Drug Deliv Rev 2013;65:2034–44.
[26] Bitar M, Salih V, Mudera V, Knowles JC, Lewis MP. Soluble phosphate glasses: in vitro studies using human cells of hard and soft tissue origin. Biomaterials 2004;25:2283–92.
[27] Shah R, Ready D, Knowles JC, Hunt NP, Lewis MP. Sequential identification of a degradable phosphate glass scaffold for skeletal muscle regeneration. J Tissue Eng Regen Med 2014;8:801–10.
[28] Lee HY, Won JE, Shin US, Kim HW. Using hydrophilic ionic liquids as a facile route to prepare porous-structured biopolymer scaffolds. Mater Lett 2011;65:2114–7.
[29] Meijering E, Jacob M, Sarria JC, Steiner P, Hirling H, Unser M. Design and validation of a tool for neurite tracing and analysis in fluorescence microscopy images. Cytometry A 2004;58:167–76.
[30] Urso-Baiarda F, Grobbelaar AO. Practical nerve morphometry. J Neurosci Methods 2006;156:333–41.
[31] Fujita K, Lazarovici P, Guroff G. Regulation of the differentiation of PC12 pheochromocytoma cells. Environ Health Perspect 1989;80:127–42.
[32] Scroggs RS, Fox AP. Calcium current variation between acutely isolated adult rat dorsal root ganglion neurons of different size. J Physiol 1992;445:639–58.
[33] Matsumoto K, Sato C, Naka Y, Whitby R, Shimizu N. Stimulation of neuronal neurite outgrowth using functionalized carbon nanotubes. Nanotechnology 2010;21:115101.
[34] Kateb B, Van Handel M, Zhang L, Bronikowski MJ, Manohara H, Badie B. Internalization of MWCNTs by microglia: possible application in immunotherapy of brain tumors. NeuroImage 2007;37(Suppl. 1):S9–S17.
[35] Malarkey EB, Reyes RC, Zhao B, Haddon RC, Parpura V. Water soluble single-walled carbon nanotubes inhibit stimulated endocytosis in neurons. Nano Lett 2008;8:3538–42.
[36] Kagan VE, Konduru NV, Feng W, Allen BL, Conroy J, Volkov Y, et al. Carbon nanotubes degraded by neutrophil myeloperoxidase induce less pulmonary inflammation. Nat Nanotechnol 2010;5:354–9.
[37] Bhirde AA, Patel S, Sousa AA, Patel V, Molinolo AA, Ji Y, et al. Distribution and clearance of PEG–single-walled carbon nanotube cancer drug delivery vehicles in mice. Nanomedicine 2010;5:1535–46.
[38] Shi Kam NW, Jessop TC, Wender PA, Dai H. Nanotube molecular transporters: internalization of carbon nanotube–protein conjugates into Mammalian cells. J Am Chem Soc 2004;126:6850–1.
[39] Nazhat SN, Neel EA, Kidane A, Ahmed I, Hope C, Kershaw M, et al. Controlled microchannelling in dense collagen scaffolds by soluble phosphate glass fibers. Biomacromolecules 2007;8:543–51.
[40] Brauer DS, Russel C, Vogt S, Weisser J, Schnabelrauch M. Degradable phosphate glass fiber reinforced polymer matrices: mechanical properties and cell response. J Mater Sci Mater Med 2008;19:121–7.
[41] Behan BL, DeWitt DG, Bogdanowicz DR, Koppes AN, Bale SS, Thompson DM. Single-walled carbon nanotubes alter Schwann cell behavior differentially within 2D and 3D environments. J Biomed Mater Res A 2011;96:46–57.
[42] Yu W, Jiang X, Cai M, Zhao W, Ye D, Zhou Y, et al. A novel electrospun nerve conduit enhanced by carbon nanotubes for peripheral nerve regeneration. Nanotechnology 2014;25:165102.
[43] Mottaghitalab F, Farokhi M, Zaminy A, Kokabi M, Soleimani M, Mirahmadi F, et al. A biosynthetic nerve guide conduit based on silk/SWNT/fibronectin nanocomposite for peripheral nerve regeneration. PLoS ONE 2013;8:e74417.
[44] Ryoo SR, Kim YK, Kim MH, Min DH. Behaviors of NIH-3T3 fibroblasts on graphene/carbon nanotubes: proliferation, focal adhesion, and gene transfection studies. ACS Nano 2010;4:6587–98.
[45] Matsumoto K, Shimizu N. Activation of the phospholipase C signaling pathway in nerve growth factor-treated neurons by carbon nanotubes. Biomaterials 2013;34:5988–94.
[46] Hwang JY, Shin US, Jang WC, Hyun JK, Wall IB, Kim HW. Biofunctionalized carbon nanotubes in neural regeneration: a mini-review. Nanoscale 2013;5:487–97.
[47] Kim YG, Kim JW, Pyeon HJ, Hyun JK, Hwang JY, Choi SJ, et al. Differential stimulation of neurotrophin release by the biocompatible nano-material (carbon nanotube) in primary cultured neurons. J Biomater Appl 2014;28:790–7.
[48] Daly WT, Yao L, Abu-rub MT, O'Connell C, Zeugolis DI, Windebank AJ, et al. The effect of intraluminal contact mediated guidance signals on axonal mismatch during peripheral nerve repair. Biomaterials 2012;33:6660–71.
[49] Cao J, Xiao Z, Jin W, Chen B, Meng D, Ding W, et al. Induction of rat facial nerve regeneration by functional collagen scaffolds. Biomaterials 2013;34:1302–10.
[50] Alvarez Z, Castano O, Castells AA, Mateos-Timoneda MA, Planell JA, Engel E, et al. Neurogenesis and vascularization of the damaged brain using a lactate-releasing biomimetic scaffold. Biomaterials 2014;35:4769–81.
[51] Al-Jamal KT, Gherardini L, Bardi G, Nunes A, Guo C, Bussy C, et al. Functional motor recovery from brain ischemic insult by carbon nanotube-mediated siRNA silencing. Proc Natl Acad Sci USA 2011;108:10952–7.
[52] Moon SU, Kim J, Bokara KK, Kim JY, Khang D, Webster TJ, et al. Carbon nanotubes impregnated with subventricular zone neural progenitor cells promotes recovery from stroke. Int J Nanomed 2012;7:2751–65.
[53] Mendler L, Pinter S, Kiricsi M, Baka Z, Dux L. Regeneration of reinnervated rat soleus muscle is accompanied by fiber transition toward a faster phenotype. J Histochem Cytochem 2008;56:111–23.
[54] Matsumoto K, Sato C, Naka Y, Kitazawa A, Whitby RL, Shimizu N. Neurite outgrowths of neurons with neurotrophin-coated carbon nanotubes. J Biosci Bioeng 2007;103:216–20.
[55] Thompson BC, Chen J, Moulton SE, Wallace GG. Nanostructured aligned CNT platforms enhance the controlled release of a neurotrophic protein from polypyrrole. Nanoscale 2010;2:499–501.